

## Structure and properties of $C_{60}$ dimers by generalized tight-binding molecular dynamics

Madhu Menon and K.R. Subbaswamy

*Department of Physics and Astronomy, University of Kentucky, Lexington, Kentucky 40506-0055*

Majid Sawtarie

*Department of Physics, Bethany College, Bethany, West Virginia 26032*

(Received 27 July 1993; revised manuscript received 25 January 1994)

Recent Raman-scattering investigations of visible- or ultraviolet-irradiated solid  $C_{60}$  film have revealed that the film consists of photopolymerized fullerene molecules with covalent intermolecular bonding in contrast to the weak van der Waals type bonding found in the crystal. In this report various  $C_{60}$  dimer geometries are studied to determine the most stable dimer configuration, using a recently developed generalized tight-binding molecular-dynamics technique. Comparison of calculated properties with experimental results strongly suggests that the linkage between  $C_{60}$  monomer units is across parallel double bonds reforming into a four-sided ring, giving a “dumbbell” structure.

The discovery of the  $C_{60}$  molecule<sup>1</sup> and other stable fullerenes has generated considerable interest in pure carbon compounds. This has led to extensive studies of fullerene-based carbon solids.<sup>2</sup> The molecules in solid  $C_{60}$  form a face centered cubic lattice (fcc) at room temperature with weak van der Waals type bonding between the molecules.<sup>3,4</sup>

In a recent paper by Rao *et al.*,<sup>5</sup> it was reported that exposure to visible or ultraviolet (UV) light causes solid  $C_{60}$  to polymerize, where the molecules cross link via covalent bonds. After phototransformation the solid  $C_{60}$  film was found to be no longer soluble in toluene. Raman-scattering studies<sup>6</sup> have found Ar-ion laser radiation to initiate an irreversible transformation of fcc  $C_{60}$  to a different solid phase with a richer Raman spectrum. Further, Raman-scattering studies of the polymeric phase revealed a new Raman-active mode at  $116\text{ cm}^{-1}$ , which was identified with an intermolecular vibrational mode.<sup>5,6</sup> While the pristine spectra for the solid  $C_{60}$  exhibit primarily intramolecular modes (ten Raman-active modes of  $A_g$  and  $H_g$  symmetry and four IR active modes of  $F_{1u}$  symmetry), consistent with the weak intermolecular interaction, the phototransformed phase was found to exhibit many more lines indicating a lowering of the icosahedral symmetry. Furthermore, the laser desorption mass spectrum of a  $C_{60}$  film phototransformed with UV-visible radiation revealed a succession of 20 regularly spaced clear peaks in the vicinity of  $C_{120}$ ,  $C_{180}$ , and so on with diminishing intensities.<sup>5</sup> Based on these observations, the authors of Ref. 5 proposed that a 2+2 cyclo addition photochemical reaction<sup>7</sup> had taken place where parallel double bonds from adjacent  $C_{60}$  molecules were broken and reformed as a four-sided ring.

In this paper, we report on the investigation of various possible covalent  $C_{60}$  dimer bonding configurations to determine the most stable bonding geometry using a recently developed generalized tight-binding molecular dynamics technique.<sup>8,9</sup> This technique has been applied

earlier to obtain equilibrium geometries for small silicon clusters,<sup>9</sup> in good agreement with *ab initio* results<sup>10,11</sup> for the lowest energy structures of silicon clusters of size up to  $N = 10$  (for which *ab initio* results are available). The present method has also been used to obtain equilibrium geometries, bond lengths, and cohesive energies for carbon clusters.<sup>12</sup> The results obtained for small clusters ( $N \leq 10$ ) are again in good agreement with available *ab initio* results.<sup>13</sup> In obtaining this agreement, the two disposable parameters appearing in the bond counting term were determined such that the total energies for  $C_2$  and  $C_3$  agreed with experimental values. Simulations of bulklike diamond with a large cluster has produced the well known  $2 \times 1$  reconstruction for the (001) face.<sup>12</sup> The bond lengths for bulklike diamond and graphitic structures are also in excellent agreement with experiments. The present method has also been used successfully to predict the lowest energy configuration for an oxygen atom chemisorbed on  $C_{60}$ .<sup>8,14</sup> Our prediction that this happens for the “epoxide” structure has been confirmed experimentally.<sup>15,16</sup>

The method is based on van Schilfgaarde and Harrison's<sup>17,18</sup> generalization of total energy calculations in tight-binding theory by explicitly incorporating nonorthogonality of the atomic orbitals. The corresponding generalization of the force calculations using the Hellmann-Feynman theorem allows us to perform molecular dynamics for covalent systems with nontetrahedral and multicoordinated structures without invoking any cutoff in the interactions. The electronic tight-binding parameters used here for carbon are generated using Harrison's<sup>19</sup> universal parameter scheme and are given in Ref. 12. The force evaluation involves only two disposable parameters that are fixed by the bond length and vibrational frequency of the carbon dimer.<sup>12</sup> Thus, there are no adjustable parameters for larger-sized clusters.

It is well known that the  $C_{60}$  molecules in a solid are

free to spin about randomly oriented axes centered on fcc lattice positions.<sup>2</sup> This is due to the fact that intermolecular interactions are weak van der Waals type and the individual molecules have very high symmetry ( $I_h$ ). Since the molecules in the solid are free to rotate, all possible relative orientations are possible in the initial stages of photopolymerization. With this in mind we do a detailed computational analysis of covalent bonding between  $C_{60}$  dimers by considering the following possible relative orientations as the initial configuration in our molecular dynamics relaxations:  $C_{60}$  units facing each other with the hexagonal edges closest to each other in parallel (1) or perpendicular (2) orientations of the double bonds; the pentagonal edges parallel to each other (3); the pentagonal faces of the dimers facing each other in an eclipsed (4) or staggered (5) geometry; hexagonal faces parallel (6); the corners of the units as the closest approach (7); the corner of one  $C_{60}$  near a bridge site over the double bond of the other molecule (8); the corner of one  $C_{60}$  over the center of a hexagonal face of the other (9); and the  $C_{58}$ - $C_2$ - $C_{60}$  geometry that was discussed as a possible alternative linkage in Ref. 5 and later rejected by the same authors (10). In all our simulations the initial configurations were chosen in such a way that the  $C_{60}$  dimers were within covalent bonding range of each other ( $\approx 2$  Å). Damped molecular dynamics relaxation was then performed by removing 1% of each velocity at each time step. No symmetry restriction is imposed while the optimization is being carried out. The process is stopped when the largest velocity component of any atom falls below 54 m/s (corresponding to a temperature of about 10 K).<sup>9</sup>

In Figs. 1 and 2 we show the initial and final configurations from our molecular dynamics relaxation for two different starting geometries (7 and 8, respectively). In both cases, the final geometry is the same, which is in fact the most stable relaxed geometry obtained. The initial configurations were taken so as not to bias them in

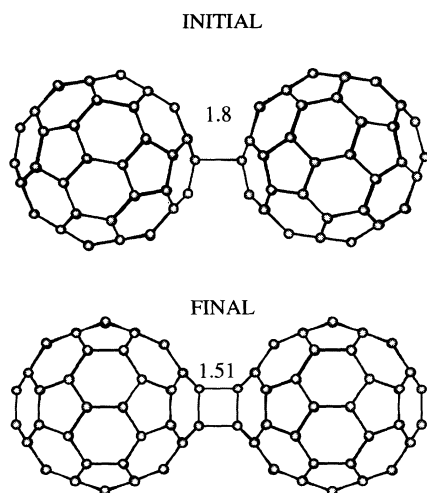


FIG. 1. Initial and final configurations of molecular-dynamics relaxation. The final structure shown is the most stable found in our optimization.

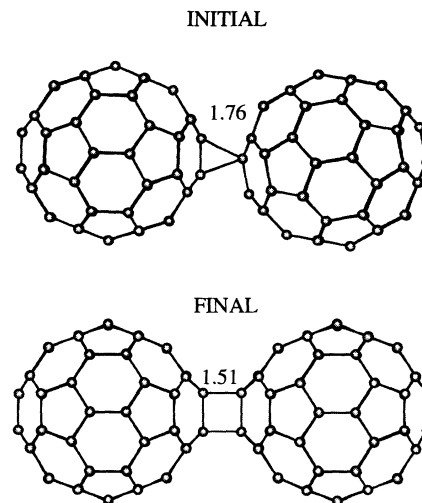


FIG. 2. Same as Fig. 1, but for a different starting geometry.

favor of symmetric bonding. The final geometry shows a “dumbbell” structure, with almost all the deviations from the perfect icosahedral symmetry confined to the nearest and next-nearest carbon atoms surrounding the four atoms participating in the interball bonding. It exhibits  $D_{2h}$  symmetry. The four atoms involved in the interball linkage form the vertices of a square of side 1.51 Å. In Table I the relative total energies are listed for all the relaxed structures considered here.

The starting geometry 2 gave no bonding and, in fact, led to a repulsion between the balls. The geometry 3 which is similar to 1 was found to be about 1 eV higher in energy than the relaxed structure shown in Fig. 1. Several starting geometries [e.g., (4, 5, 6, and 9)] led to relaxed structures with substantially higher energies (see Table I). The relaxed  $C_{58}$ - $C_2$ - $C_{60}$  geometry (10), which involves the breaking of the cage framework, is found to be significantly higher in energy than the dumbbell (by 4.8 eV). Subsequent experimental analysis by the authors of Ref. 5 has ruled out this structure. Considering the extensive sampling of initial orientations, it is reasonable

TABLE I. Relative energies for various  $C_{60}$  dimer configurations with respect to the “dumbbell.”

Structure	Relative total energies $\Delta E$ (eV)
1	0.0
2	no bonding
3	0.96
4	5.76
5	2.16
6	2.16
7	unstable
8	unstable
9	5.76
10	4.80
Two isolated $C_{60}$	-0.60

to conclude that the fourfold cyclic linkage shown in Figs. 1 and 2 is the minimum energy configuration.

In Figs. 3(a) and 3(b) we show the energy levels in the vicinity of the Fermi level for an isolated  $C_{60}$  and the dumbbell (our lowest energy configuration for the dimer). An isolated  $C_{60}$  has a fivefold degenerate highest occupied molecular orbital and a threefold degenerate lowest unoccupied molecular orbital with a gap of 1.10 eV. As seen in Fig. 3(b), the formation of the dimer has removed the degeneracy of energy levels near the Fermi level as a consequence of the lowered symmetry. The narrowing of the optical gap is consistent with the observed darkening of the photoinduced film.<sup>5</sup>

The present method can also be easily used to obtain vibrational frequencies for clusters by explicitly constructing the dynamical matrix. For a  $C_{60}$  molecule we obtained a radial "breathing mode" ( $A_g$  symmetry) frequency of  $503\text{ cm}^{-1}$ .<sup>21</sup> The frequency for the "pentagonal-pinch" mode (also of  $A_g$  symmetry) was determined to be  $1597\text{ cm}^{-1}$ .<sup>21</sup> The experimental values for these modes are  $496\text{ cm}^{-1}$  and  $1470\text{ cm}^{-1}$ , respectively.<sup>20</sup> This agreement is excellent when we consider that the parameters used in our calculations were fitted in the dimer regime<sup>12</sup> and this gives us reason to believe in the reliability of the method when it is used to estimate vibrational frequencies for other clusters.

We have also determined the vibrational mode frequencies for the dumbbell by explicitly constructing the dynamical matrix. As expected, most of the modes are easily recognized as monomer derived, with all degeneracies removed. There are six additional modes associated with intermolecular vibrations. In Fig. 4 we show the atomic displacement patterns for one Raman-active mode at  $101\text{ cm}^{-1}$  (top panel: a symmetric distortion of the dumbbell), and for one infrared active mode at  $228\text{ cm}^{-1}$  (bottom panel: a libration mode). Experimentally a new mode at  $116\text{ cm}^{-1}$  has been observed in the Raman spectrum of the photopolymerized  $C_{60}$  film,<sup>5</sup> which is in good agreement with the calculated frequency of the

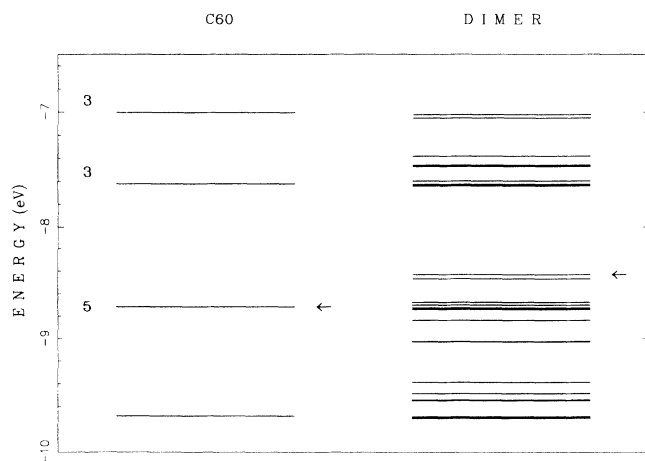


FIG. 3. Energy levels in the vicinity of the Fermi level for an isolated  $C_{60}$  and the dumbbell (our lowest energy configuration for the dimer).

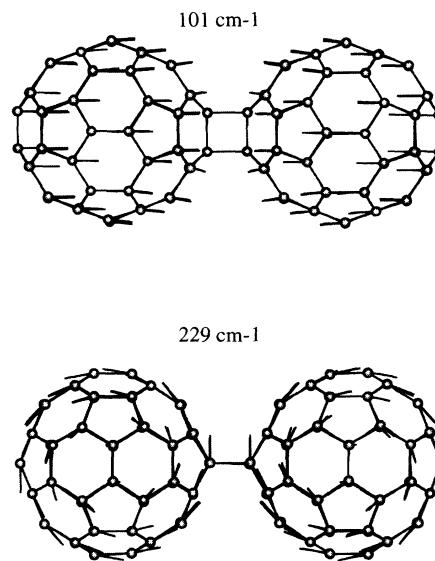


FIG. 4. Vibrational displacement patterns for the dumbbell for a symmetric distortion mode at  $104\text{ cm}^{-1}$  (upper panel) and for a libration mode at  $227\text{ cm}^{-1}$ .

distortion mode displayed in Fig. 4.

In Fig. 5 we show the low frequency vibrational spectra for the dumbbell (top) and the isolated  $C_{60}$  (bottom). The lowering of the perfect icosahedral ( $I_h$ ) symmetry for the dimer gives rise to a removal of degeneracies of vibrational modes present in the isolated  $C_{60}$ , resulting in many additional modes shown in the figure. The intermolecular stretch and librational modes dominate the lower end of the spectrum for the dimer.

We find the dimer formation to be slightly endothermic ( $\approx 0.6\text{ eV}$ ). We have estimated an upper bound to the dissociation barrier for the dimers, starting with the minimum geometry shown in Fig. 1, by calculating the

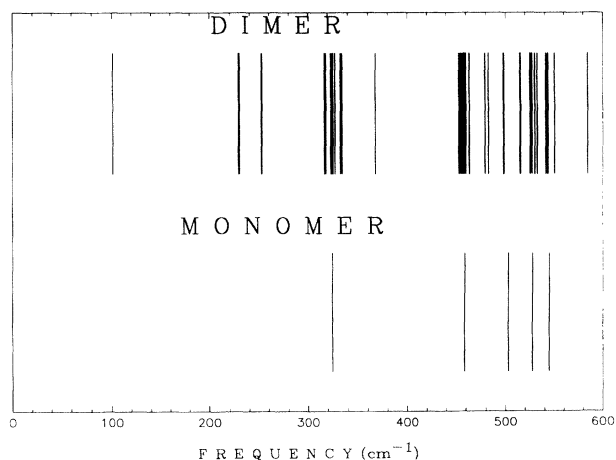


FIG. 5. Low frequency vibrational spectra for the dumbbell (top) and the isolated  $C_{60}$  (bottom). The intermolecular stretch and librational modes dominate the lower end of the spectrum for the dimer.

total energy when the interball separation is increased while keeping all other bonds and angles frozen. From this and other supplementary calculations we estimate the barrier to be in the range of 2–4 eV.

In conclusion, we have investigated the relative stabilities of various dimer configurations of the C<sub>60</sub> molecule using a recently developed generalized tight-binding molecular dynamics scheme which has yielded results for equilibrium geometries for small carbon clusters in complete agreement with *ab initio* work. Comparison of calculated properties of the dimer with experimental results on photopolymerized C<sub>60</sub> films strongly suggests that the linkage between C<sub>60</sub> monomer units in the polymer is across parallel double bonds of the fullerene molecules, reforming into a four-sided ring, with the dimer resembling a dumbbell structure.

*Note added.* Recently, another work on the bonding of two C<sub>60</sub> molecules based on geometry optimization employing MNDO and tight-binding methods has appeared.<sup>22</sup> The conclusion of these authors are essen-

tially the same as ours in that they also find the “dumbbell” to be the most stable among various bonding configurations they considered. Their intermolecular stretching frequency of 81 cm<sup>-1</sup> determined using an orthogonal tight-binding scheme is much smaller when compared to the experimental value of 116 cm<sup>-1</sup> reported by the authors of Ref. 5. The orthogonal tight-binding scheme is known to be unreliable when used to determine vibrational frequencies. Our nonorthogonal scheme remedies these shortcomings by explicitly incorporating the overlap interactions and gives much improved agreement with experiment as described in Refs. 9 and 12.

We thank Peter Eklund and A. M. Rao (U. of Kentucky) for very helpful discussions. This research was supported in part by USDOE Contract No. DE-FC22-90PC90029, by NSF Grant No. EHR 91-08764, and by the University of Kentucky Center for Computational Sciences. One author (M.S.) acknowledges financial support from the Pew Charitable Trust.

- 
- <sup>1</sup> H. W. Kroto, J. R. Heath, S. C. O'Brien, R. F. Curl, and R. E. Smalley, *Nature* (London) **318**, 162 (1985).
  - <sup>2</sup> See the special issue, *Acc. Chem. Res.* **25**, 98 (1992), for a review of fullerene-based solids.
  - <sup>3</sup> P. A. Heiney *et al.*, *Phys. Rev. Lett.* **66**, 2911 (1991).
  - <sup>4</sup> P. A. Heiney *et al.*, *Phys. Rev. Lett.* **67**, 1468 (1991).
  - <sup>5</sup> A. M. Rao *et al.*, *Science* **259**, 955 (1993).
  - <sup>6</sup> P. Zhou *et al.*, *Appl. Phys. Lett.* **60**, 2871 (1992).
  - <sup>7</sup> J. D. Coyle, *Introduction to Organic Photochemistry* (Wiley, New York, 1986), p. 61.
  - <sup>8</sup> M. Menon and K. R. Subbaswamy, *Phys. Rev. Lett.* **67**, 3487 (1991).
  - <sup>9</sup> M. Menon and K. R. Subbaswamy, *Phys. Rev. B* **47**, 12 754 (1993).
  - <sup>10</sup> K. Raghavachari, *J. Chem. Phys.* **84**, 5672 (1986).
  - <sup>11</sup> K. Raghavachari, and C. M. Rohlfing, *J. Chem. Phys.* **89**, 2219 (1988).
  - <sup>12</sup> M. Menon, K. R. Subbaswamy, and M. Sawtarie, *Phys. Rev. B* **48**, 8398 (1993).
  - <sup>13</sup> K. Raghavachari and J. S. Binkley, *J. Chem. Phys.* **87**, (1987) 2191.
  - <sup>14</sup> M. Menon and K. R. Subbaswamy, *Chem. Phys. Lett.* **201**, 321 (1993).
  - <sup>15</sup> K. M. Creegan, J. L. Robbins, W. K. Robbins, J. M. Millar, R. D. Sherwood, P. J. Tindall, D. M. Cox, A. B. Smith III, J. P. McCauley, Jr., D. R. Jones, and R. T. Gallagher, *J. Am. Chem. Soc.* **114**, 1103 (1992).
  - <sup>16</sup> Y. Elemes, S. K. Silverman, C. Sheu, M. Kao, C.S. Foote, M. M. Alvarez, and R. L. Whetten, *Angew. Chem. Int. Ed. Engl.* **31**, 351 (1992).
  - <sup>17</sup> M. van Schilfgaarde and W. A. Harrison, *J. Phys. Chem. Solids* **46** (9), 1093 (1985).
  - <sup>18</sup> M. van Schilfgaarde and W. A. Harrison, *Phys. Rev. B* **33**, 2653 (1986).
  - <sup>19</sup> *Electronic Structure and the Properties of Solids*, edited by W. Harrison (Freeman Press, San Francisco, 1980).
  - <sup>20</sup> D. S. Methune, G. Meijer, W. C. Tang, H. J. Rosen, W. G. Golden, H. Seki, C. A. Brown, and M. S. De Vries, *Chem. Phys. Lett.* **179**, 181 (1991).
  - <sup>21</sup> M. Menon, J. Yang, and K. R. Subbaswamy (unpublished).
  - <sup>22</sup> D. L. Strout *et al.*, *Chem. Phys. Lett.* **214**, 576 (1993).

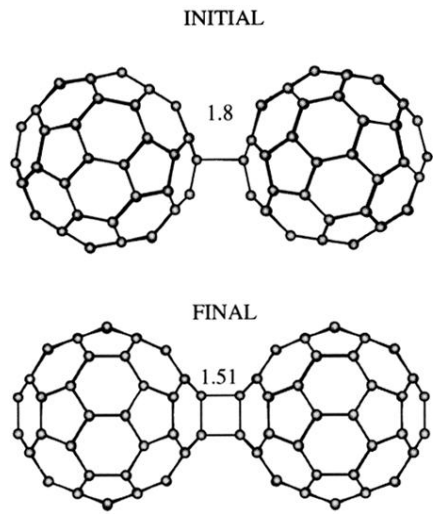


FIG. 1. Initial and final configurations of molecular-dynamics relaxation. The final structure shown is the most stable found in our optimization.

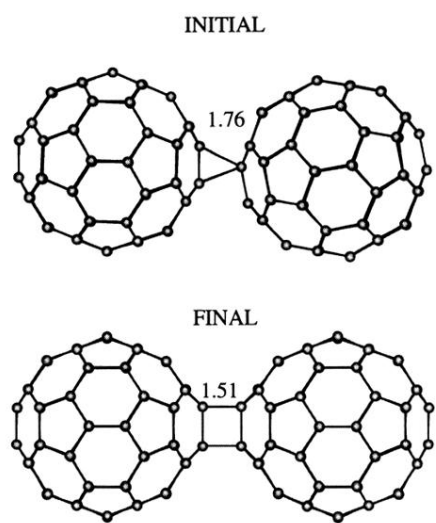


FIG. 2. Same as Fig. 1, but for a different starting geometry.

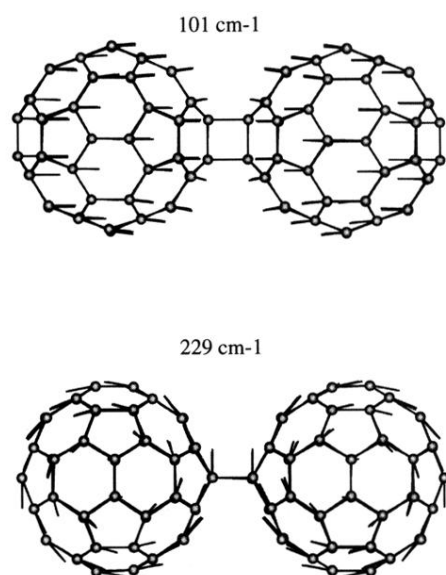


FIG. 4. Vibrational displacement patterns for the dumbbell for a symmetric distortion mode at  $104\text{ cm}^{-1}$  (upper panel) and for a libration mode at  $227\text{ cm}^{-1}$ .